4-Nonylphenol induces autophagy and attenuates mTOR-p70S6K/4EBP1 signaling by modulating AMPK activation in Sertoli cells

Duan P[1], Hu C[2], Quan C[3], Yu T[3], Huang W[3], Chen W[3], Tang S[3], Shi Y[4], Martin FL[5], Yang K[6]

[1]*MOE (Ministry of Education) Key Lab of Environment and Health, Department of Occupational and Environmental Health, Tongji Medical College, Huazhong University of Science and Technology, Wuhan 430030, China; Research Center for Environment and Health, Hubei University of Medicine, Shiyan 442000, China*

[2]*Department of Clinical Laboratories, Taihe Hospital, Hubei University of Medicine, Shiyan 442000, China*

[3]*MOE (Ministry of Education) Key Lab of Environment and Health, Department of Occupational and Environmental Health, Tongji Medical College, Huazhong University of Science and Technology, Wuhan 430030, China*

[4]*Department of Epidemiology and Health Statistics, School of Public Health, Medical College, Wuhan University of Science and Technology, Wuhan 430030, China*

[5]*School of Pharmacy and Biomedical Sciences, University of Central Lancashire, Preston PR1 2HE, UK*

[6]*MOE (Ministry of Education) Key Lab of Environment and Health, Department of Occupational and Environmental Health, Tongji Medical College, Huazhong University of Science and Technology, Wuhan 430030, China. Electronic address: yangkd@mails.tjmu.edu.cn*

ABSTRACT

The estrogenic chemical 4-nonylphenol (NP) is known to impair testicular devolopment and spermatogenesis in rodents. The objective of this study was to explore the effects of NP on autophagy induction and AMPK-mTOR signaling pathway in Sertoli cells (SCs), which are the "nursemaid cells" for meiosis of spermatocytes. In this study we exposed 7-week-old male rats to NP by intra-peritoneal injection at 0, 20, 50 or 100 mg/kg body weight/2 days for 20 consecutive days. Our results showed that exposure to NP dose-dependently induces the formation of autophagosomes in SCs, increases the expression of Beclin-1, the conversion of LC3-I to LC3-II and the mRNA expression of Atg3, Atg5, Atg7 and Atg12 in testis, and these effects are concomitant with the activation of AMPK, and the suppression of TSC2-mTOR-p70S6K/4EBP1 signaling cascade in testis. Furthermore, 10 μM Compound C or AMPKα1 siRNA pre-treatment effectively attenuated autophagy and reversed AMPK-mTOR-p70S6K/4EBP1 signaling in NP-treated SCs. Co-treatment with 1 mM AICAR remarkably strengthened NP-induced autophagy and mTOR inhibition in SCs. Together, these data suggest that NP stimulates Sertoli cell autophagy and inhibits mTOR-p70S6K/4EBP1 activity through AMPK activation, which is the potential mechanism responsible for the regulation of testis function and differentiation following NP exposure.

Keywords: 4-nonylphenol, Sertoli cells**,** Autophagy**,** AMPK**,** mTOR-p70S6K/4EBP1

1. Introduction

4-Nonylphenol (NP) is a primary breakdown product of nonylphenol ethoxylate (NPE), nonionic surfactant widely employed in domestic, industrial and agricultural applications (Lepretti et al. 2015;

Liu et al. 2015). NP has been detected in surface water, groundwater, atmosphere, soils and human foodstuffs in various countries around the world, suggesting widespread human exposure (Vidal-Linan et al. 2015). Due to its hydrophobic nature, NP tends to adsorb on lipid-rich particles and bio-accumulate in organisms, concentrating in the food chain and enhancing human exposure to NP (Vidal-Linan et al. 2015). NP, which has in recent years been reported to structurally and functionally mimic oestrogens and to exert oestrogen-like activities, has become one of the most commonly encountered environmental endocrine disruptors (EDs) (Lyons et al. 2014). Significantly, EDs has been suggested to exhibit adverse effects not only on endocrine homeostasis but also on the male reproductive function (Guerrero-Bosagna and Skinner 2014). Especially the issue of male infertility of the xenoestrogen NP is increasingly a matter of public concern (Chen et al. 2013; Verderame and Limatola 2015).

Accumulating studies have revealed that NP toxicity induces oxidative stress through the generation of ROS and stimulates apoptosis in a variety of cell types, including human embryonic stem cells, TM4 SCs and testicular SCs (Choi et al. 2014; Gong et al. 2009; Kim et al. 2006; Kuo et al. 2012; Zhang et al. 2014). NP activates endoplasmic reticulum stress response, Fas/FasL, MAPKs, Akt and JNK signaling pathways, resulting in changes in cell survival, cell cycle progression and apoptosis (Choi et al. 2014; Duan et al. 2016c; Lepretti et al. 2015; Liu et al. 2015; Yao et al. 2005). Importantly, our previous study outlined that NP treatment triggers Sertoli cell (SC) autophagy, probably through the ROS-mediated AMPK-mTOR pathway (Duan et al. 2016c). Additionally, NP exposure is shown to increase oxidative stress and germ cell apoptosis in testis, to cause seminiferous tubule degeneration and to reduce hormone secretion, consequently impairing sperm parameters, capacitation and morphology (Duan et al. 2016a; Duan et al. 2016b; Lu et al. 2014; McClusky et al. 2007). Although increasing evidence suggests that autophagy activity may play an important function in the pathogenesis of male reproductive toxicity (Han et al. 2015), no information regarding NP effects on autophagy induction *in vivo* is currently available.

The mammalian target of rapamycin (mTOR) is an evolutionarily conserved serine/threonine kinase that performs critical functions of the regulation of cell growth and cell metabolism by responding to changes in nutrients, growth factors and cellular energy status (Albert and Hall 2015; Yue et al. 2015). Accordingly, mTOR has been considered as a central signaling node that adapts metabolism to environmental and metabolic variations (Albert and Hall 2015). The latest research has indicated that mTOR-p70S6K/4EBP1 signaling regulates spermatogonia proliferation and spermatogenesis through multiple signal transduction pathways (Jesus et al. 2015; Lu et al. 2015). mTOR exists in two large protein complexes: mTOR complex 1 (mTORC1) and 2 (mTORC2), each with unique functions and downstream targets. In particular, mTORC1 integrates various stimuli and signaling networks to coordinate autophagy and cell metabolism (Kim et al. 2015). It is well established that cellular autophagy is negatively regulated by mTOR and phosphorylation of mTOR at Ser2448 is an activator of mTORC1 (Yamamoto et al. 2014). Moreover, mTOR regulates protein synthesis by phosphorylating downstream targets p70S6k and 4EBP1, at least partly controlling spermatogonial differentiation (Busada et al. 2015; Churchward-Venne et al. 2012).

The AMP-activated protein kinase (AMPK) is a key sensor and regulator of energy status that, when activated by metabolic stress, coordinate multiple signaling pathways to maintain cellular energy homeostasis (Hardie 2015). Intriguingly, abundant studies have demonstrated that AMPK has the ability to stimulate autophagy by inhibiting the mTOR signaling via phosphorylation of the tuberous sclerosis complex 2 (TSC2) (Wu et al. 2015). Additionally, previous study of Tanwar et al has

suggested that aberrant AMPK-mTOR signaling causes disruption of SC polarity and spermatogenesis (Tanwar et al. 2012). Well-coordinated AMPK-mTOR signaling is essential for SCs functions and survival (Riera et al. 2012; Tanwar et al. 2012). Thus, it is important to elucidate possible contribution of AMPK-mTOR signaling to NP-induced rat SC toxicity.

SCs, one of the somatic cells of the testis, are critical regulators of spermatogenesis as their main functions are to control germ cell differentiation in the seminiferous tubules, to provide physical and nutritional support for the developing sperm and to form the blood-testis-barrier (Escott et al. 2014; Hai et al. 2014). It is now well established that the in vitro study of SC physiology is a useful model to disclose deleterious effects of toxicant exposure to male fertility and to probe the molecular mechanisms that regulate spermatogenesis (Li et al. 2016; Reis et al. 2015). Therefore, in the present study, we established both the SC and rat models to determine the effect of NP on the activity of autophagy in SCs and to explore its underlying mechanisms in view of the intriguing role of AMPK-mTOR signaling pathway.

2. Materials and methods

2.1. Reagents and antibodies

NP (CAS no. 84852-15-3; Mixture of isomers; empirical formula $C_{15}H_{24}O$; molecular weight 220.35) with 99% analytical standard was purchased from ACROS Organics (UK). Foetal bovine serum (FBS) was purchased from Hangzhou Evergreen Biological Engineering Company (China). Type I collagenase and Lipofectamine LTX transfection reagent were purchased from Invitrogen (Grand Island, NY, USA). Dulbecco's modified Eagle's medium (DMEM) containing a high concentration of glucose was purchased from Hyclone Company (Logan, UT, USA). Trypsin, dimethyl sulfoxide (DMSO) and phalloidin were purchased from Sigma-Aldrich (St. Louis, MO, USA). Horseradish peroxidase (HRP)-conjugated goat anti-rabbit secondary antibody and Compound C were purchased from Santa Cruz Biotechnology (Santa Cruz, USA). 4,6-Diamidino-2-phenylindole (DAPI), penicillin-streptomycin solution and BCA protein assay kit were purchased from Beyotime Company of Biotechnology (Shanghai, China). FSHR and 5-aminoimidazole-4-carboxamide riboside (AICAR) were purchased from Abcam (Cambridge, MA). OPTI-MEM was obtained from GIBCO (Maryland, USA). TRIzol® Reagent and Platinum® SYBR® Green qPCR SuperMix-UDG kit were purchased from Invitrogen (Carlsbad, CA). Revert Aid First Strand cDNA Synthesis kit was purchased from Fermentas UAB (Vilnius, Lithuania). Rabbit monoclonal antibodies against β-actin, LC3, Beclin-1, AMPK, p-AMPK^{Thr172}, TSC2, p-TSC2^{Thr1462}, mTOR, p-mTOR^{ser2448}, 4EBP1, p-4EBP1$^{Thr37/Thr45}$, p70S6K, and p-p70S6K^{Thr389} were purchased from Cell Signaling Technology (MA, USA).

2.2. Animal treatments and tissue preparation

All experimental protocols using animals were approved by the Animal Care and Use Committee of the Tongji Medical College (Wuhan, China), and were performed according to the guidelines of the National Institutes of Health of China. Twenty-four Sprague-Dawley (SD) rats (male, 6-week-old) were obtained from Tongji Medical College Animal Center (Wuhan, China), and were housed in a controlled animal room (room temperature: $23 \pm 3℃$; relative humidity, $55 \pm 20\%$; lighting cycle, 12 h

light/12 h dark). Rats were allowed free access to purified water and standard rodent chow. After 1 week of acclimatization, rats were randomly divided into four groups of 6 rats each: three NP treatment groups and a control group. The NP-treated groups of rats were administered NP (25, 50 or 100 mg/kg body weight) dissolved in corn oil, by intra-peritoneal injection every other day for 20 consecutive days. Control rats were injected with equal volumes of corn oil (5 mL/kg body weight).

After NP administration, the rats were weighed and sacrificed by decapitation. The testis were immediately removed, weighed and rinsed with ice-cold physiological saline (4°C). The dissected tissue (1×1×1 mm per specimen) from each right testis was prepared and then fixed in 2.5% glutaraldehyde in 0.1 M phosphate buffer (pH 7.4) for transmission electron microscopy. The rest testis of each rat in all groups were quickly frozen in liquid nitrogen followed by storage at -80°C until analysis.

2.3. Primary culture of Sertoli cells from 18-20-day-old rats and treatments

Primary SCs were isolated from the testes of rats (18-20 days), as at this stage the majority of the cells inside the seminiferous tubules are SCs. The procedure for the isolation of the SCs was as previously described with minor modifications (Duan et al. 2016c; Huang et al. 2016). The resulting cell suspension was resuspended with fresh DMEM containing 5% fetal bovine serum, penicillin (100 IU/ml) and streptomycin (100 IU/ml). Afterwards, single cells were counted with a hemocytometer, seeded in T75 flasks at a density of $1×10^6$ cells/mL and incubated at 37°C in a humidified atmosphere of 95% air and 5% CO_2. After 12 h incubation, the cells were washed twice (5 min each) with D-Hanks solution and treated with 20 mM pH 7.4 Tris–HCl for 5 min. The cultured medium was replaced with fresh complete medium and renewed daily. The total incubation period was 2 days prior to the indicated treatment. SCs purity was assessed by immunofluorescence staining for FSHR. Only the isolated cells with the purity of SCs >90% and good growth status were used to perform the following treatments.

NP was dissolved in DMSO as stock solution and freshly diluted with DMEM medium to different concentrations (10, 20 and 30 µM) before being added to SCs in culture. SCs were treated with vehicle alone (DMSO; 0.1%, v/v) or a series of concentrations of NP dissolved in 0.1% DMSO for 12 h. The effects of DMSO on the variables were determined in our previous study, which showed no significant differences between DMSO-treated and untreated cells (Duan et al. 2016c).

2.4. Compound C and AICAR pretreatments

Compound C was dissolved in 100% DMSO at 10 mM as storage concentration. AICAR was first dissolved in DMSO in a 100 mM stock solution. Compound C and AICAR used at the selected concentrations (Compound C: 5–10µM; AICAR: 0.5–1 mM) did not yield any significant cell damage to cultured SCs. Moreover, the effect of different doses of Compound C (5–10µM) and AICAR (0.5–1 mM) on AMPK expression was examined by Western blotting (data are not shown here). In this study, 10 µM Compound C and 1 mM AICAR were used to interfere with the activity of AMPK in vitro.

Primary cultures of SCs were pre-treated with 10 μM Compound C for 2 h, and then posttreated with the indicated doses of NP for 12 h (Compound C + NP). For AICAR pretreatment, 1 mM AICAR was applied to SCs and lasted for 2 h to enhance AMPK activity, following the addition of NP for another 12 h.

2.5. Transfection with small-interfering RNA (siRNA)

The siRNA targeting AMPKα1 (rat, sc-270142) was purchased from Santa Cruz Biotechnology, along with a control siRNA (sc-37007). The siRNA transfection experiment was performed according to the supplier's protocol. Briefly, SCs at ~60% confluency were washed once with Opti-MEM, transfected with siRNA targeting AMPKα1 combined with Lipofectamine LTX Reagent and Opti-MEM for 6 h, and then supplemented with basal growth medium for an additional 24 h. After transfection, siRNA containing media were discarded and the transfected SCs were exposed to the indicated treatments. Knocking down of protein expressions were confirmed by western blotting. SCs treated with scramble siRNA or with Lipofectamine alone were not significantly different from untreated SCs for the protein expression of AMPK and its phosphorylation (Thr172).

2.6. RNA extraction and RT-PCR

Total RNA of each sample was extracted with Trizol reagents according to the manufacturer's protocol. The extracted RNA was quantified using a BioPhotometer (Eppendorf, Germany). Only the RNA samples with 260/280 nm absorbance ratios of 1.8-2.0 were considered of acceptable purity and then used for further studies. Equal amounts of RNA (2 μg) were reverse transcribed using Revert Aid First Strand cDNA Synthesis Kit. Primer sequences used for real-time RT-PCR analysis are summarized in Table SI. RT-PCR was performed with an ABIPRISM® 7900HT Sequence Detection System (Applied Biosystems) using Platinum® SYBR® Green qPCR SuperMix-UDG with ROX. The mRNA expression is expressed as the ratio between the target gene and β-actin gene expression.

2.7. Western blot analysis

At the end of the designated treatments, each sample completely lysed in RIPA lysis buffer and then centrifuged at 12 000 rpm for 10 min at 4°C. Debris was removed and protein content was quantified using the BCA Protein assay kit according to the manufacturer's instructions. Western blotting was performed as previously described (Qi et al. 2014). Briefly, protein samples (20 μg per lane) were separated by electrophoresis on sodium dodecyl sulphate polyacrylamide gels and transferred to nitrocellulose membranes by electrophoresis and Trans-Blot Turbo systems (Bio–Rad). The membranes were then blocked in 5% non-fat milk in Tris-buffered saline containing 0.05% Tween 20 for 2 h at room temperature. Blots were probed with primary antibodies overnight at 4°C, washed with four changes of TBST and then incubated with the appropriate HRP-conjugated secondary antibodies for 1 h at room temperature. After washing twice with washing buffer, the immunoreactive bands were visualized by ECL Plus Western blotting detection system. The band intensities were quantified using Quantity One software and normalized by β-actin levels.

2.8. Immunofluorescence staining

SCs were plated in 4-well chamber slides and exposed to indicated culture conditions. After treatment, SCs were fixed with 4% paraformaldehyde at room temperature for 30 min, and then permeabilized with 0.1% Triton X-100 in TBS for 5 min. Blocking was performed with 10% bovine serum albumin and 1% goat serum in PBS at 37°C for 30 min. After the blocking solution was removed, SCs were incubated with rabbit monoclonal antibodies against β-actin, p-AMPK^{Thr172}, AMPK and p-mTOR^{ser2448} for 1 h at 37°C and then washed with 0.1% BSA in PBS three times. Thereafter SCs were incubated with HRP-conjugated goat anti-rabbit secondary antibody diluted in blocking solution for 1 h at 37°C. The nuclei were additionally incubated 5 min in DAPI (1 μg/mL). The labelled targets in SCs were detected under a confocal microscope (Olympus, Tokyo, Japan).

For phalloidin staining of the actin cytoskeleton, the permeabilized SCs were incubated with phalloidin staining solution (5 μg/mL in PBS) for 1 h at 37°C. After being stained with DAPI, SCs were detected under a confocal microscope. For reliable results, the experiments were performed in triplicate and repeated 3 times.

2.9. Statistical analysis

Data calculations and statistical analysis were performed using SPSS software version 12.0 (SPSS Inc., Chicago, IL, USA). Quantitative variables were expressed as mean ± standard deviation (SD) of at least three independent experiments. Statistical significance was determined by one-way analysis of variance (ANOVA) followed by Fisher's least significant difference (LSD), or by non-parametric tests, depending on the homogeneity of variance tested with Levene's test. For all the tests, a two-sided P <0.05 was considered statistically significant.

3. Results

3.1. NP promotes SC autophagy in rat testis

Examining the ultrastructural details of autophagosomes using TEM is the gold standard for determining autophagy. To verify the induction of SC autophagy in rat testis after NP treatment, TEM studies were performed. As shown in Fig. 1A, SCs in rats treated with NP (50 and 100 mg/kg) had a remarkable increase number of autophagosomes and autolysosomes, compared with untreated controls. The results from real-time PCR analysis showed that Beclin-1, Atg 3, Atg 5, Atg 7 and Atg 12 mRNA levels in testis were significantly elevated in response to NP administration (50 and 100 mg/kg) (Fig. 1B). Furthermore, compared with the control group, treatment with NP at concentrations of 50 to 100 mg/kg led to a significant increase in protein expression of LC3-II, Beclin-1 as well as in the LC3-II/LC3-I ratio (Fig. 1C). Altogether, these results strongly support that NP is capable of inducing SC autophagy in testicular tissues of adult male rats.

3.2. NP triggers activation of AMPKα-TSC2-mTOR-p70S6K/4EBP1 signaling pathway in rat testis

AMPK-regulated mTOR signaling pathway has been suggested to be one of the master regulators of autophagy (Wu et al. 2015; Yamamoto et al. 2014). We next investigated whether NP induces autophagy through modulation of AMPK-mTOR pathway in testis. As illustrated in Fig. 2A, the

expression of phosphorylated-AMPKα was up-regulated in a dose-dependent manner after NP administration, and that of TSC2, mTOR, p70S6K and 4EBP1 phosphorylation was dose-dependently inhibited, whereas no significant changes were observed in the expression of t-AMPKα, t-TSC2, t-mTOR, t-p70S6K and t-4EBP1 between the control and NP-treated groups (Fig. 2B). The ^{Thr172}p-AMPKα/AMPKα ratios in the rats treated with 50 and 100 mg/kg NP were much higher than those without NP treatment. Meanwhile, compared with the control group, the ratios of ^{Thr1462}p-TSC2/TSC2, ^{Ser2448}p-mTOR/mTOR, ^{Thr389}p-p70S6K/p70S6K and $^{Thr37/45}$p-4EBP1/4EBP1 were significantly decreased at NP 50 and 100 mg/kg. These results suggest that AMPK-mTOR signaling pathway may be involved in NP-induced autophagy in testis.

3.3. The AMPK inhibitor Compound C counteracts the effects of NP on AMPK-mTOR signaling pathway and autophagy

Since AMPK is a major negative regulator of mTOR pathway (Wu et al. 2015), we further studied whether NP-induced AMPK activation leads to inhibition of mTOR signaling as well as up-regulation of autophagy in SCs. Firstly, we studied the effect of Compound C, an antagonist of the AMPK signaling pathway. As shown in Fig. 3A, immunofluorescence analysis of SCs pre-treated with Compound C exhibited a remarkable decrease in AMPKα protein expression level. Western blotting analysis also showed that pre-treatment of Compound C strongly suppressed AMPKα expression and blocked the AMPKα phosphorylation stimulated by NP in SCs (Fig. 3B). SCs pre-treated with Compound C significantly lowered the phosphorylation level of AMPKα and ratio of ^{Thr172}p-AMPKα/AMPKα as compared to SCs treated with NP alone (Fig. 3C).

Furthermore, compared to the NP treated groups, TSC2, mTOR, p70S6K and 4EBP1 phosphorylation inhibition were obviously restored and ^{Thr1462}p-TSC2/TSC2, ^{Ser2448}p-mTOR/mTOR, ^{Thr389}p-p70S6K/p70S6K and $^{Thr37/45}$p-4EBP1/4EBP1 levels were significantly increased after down-regulation with Compound C for AMPK (Fig. 3C). Importantly, as the Fig. 3C shown, NP-induced conversion of LC3-I to LC3-II and up-regulation of Beclin-1 expression were almost reversed by Compound C, and there was statistical significance between the Compound C+NP (30 µM) group and the 30 µM NP-induction group, suggesting that AMPK activation is required for autophagy induced by NP in SCs.

3.4. The AMPK activator AICAR aggravates the effects of NP on AMPK-mTOR signaling and autophagy

As shown in Fig. 4A, immunofluorescence analysis of AMPKα revealed higher levels of AMPKα in AICAR-pre-treated SCs than that in cells incubated with NP alone or without NP. Western blot analysis revealed concordant results for AMPKα protein expression (Fig. 4B). Note that the phosphorylation level of AMPKα in response to NP exposure was significantly increased by AICAR (Fig. 4C). Moreover, SCs pre-treated with AICAR had higher level of ^{Thr172}p-AMPKα/AMPKα than SCs treated with NP alone (Fig. 4C). In both NP and NP+AICAR groups, LC3-II/LC3-I and Beclin-1 levels were significantly enhanced compared to the corresponding control group. Especially, there was statistical significance between the AICAR+NP group and the NP group.

AMPK agonist obviously decreased the phosphorylation of mTOR, p70S6K and 4EBP1 in SCs treated with AICAR alone when compared with untreated controls (Fig. 4B), as well, there was statistical significance between the control group and the AICAR group when considering the ratios of ^{Ser2448}p-mTOR/mTOR, ^{Thr389}p-p70S6K/p70S6K and $^{Thr37/45}$p-4EBP1/4EBP1. Intriguingly, compared to the NP treated group, the ^{Ser2448}p-mTOR/mTOR ratio was significantly decreased after up-regulation

with AICAR for AMPK (Fig. 4C), whereas the ratios of ^{Thr389}p-p70S6K/p70S6K and $^{Thr37/45}$p-4EBP1/4EBP1 showed statistically not significant difference between the AICAR+NP group and the NP group.

3.5. AMPKα1 siRNA attenuates the effects of NP on AMPK-mTOR-p70S6K/4EBP1signaling and autophagy

To further confirm the role of AMPK in modulating autophagy induced by NP, we used siRNA to knockdown AMPKα1 expression. siRNA-transfected cells were visualized by staining with phalloidin (Fig. 5A), which displayed that siRNA against AMPKα1 somehow disrupted the cytoskeleton and the morphology of SCs when compared with the corresponding controls. However, this appeared to have no impact on our final conclusions. As indicated in Fig. 5B, silencing AMPKα in SCs successfully suppressed AMPKα protein expression and effectively diminished NP-induced AMPKα phosphorylation. Moreover, as it was expected, NP-induced up-regulation of ^{Thr172}p-AMPKα/AMPKα was notably attenuated in the presence of AMPKα1 siRNA (Fig. 5C).

In line with NP treatment, knockdown of AMPKα not only inhibited SC autophagy, as indicated by decreased conversion of LC3-I to LC3-II, but also elevated phosphorylation of the AMPK downstream targets, mTOR, p70S6K and 4EBP1 (Fig. 5B). Compared to the NP treated group, the LC3-II/LC3-I ratio was significantly decreased. Meanwhile, ^{Ser2448}p-mTOR/mTOR, ^{Thr389}p-p70S6K/p70S6K and $^{Thr37/45}$p-4EBP1/4EBP1 levels were markedly up-regulated in the siRNA+NP group (Fig. 5C). Together, these results suggest that NP, via activating AMPK-mTOR signaling, induces autophagy in SCs.

4. Discussion

There is increasing evidence that autophagy plays a regulatory role in spermatogenesis impairment targeting the injurious biochemical and molecular cascade (Wang et al. 2014b; Yefimova et al. 2013). Autophagy is a multifaceted process and is known to function either as pro-survival or pro-death signaling. Previously, we developed a SC model to investigate the potential cytotoxicity of NP on SCs; Interestingly, we found that NP induces SC autophagy (Duan et al. 2016c). This observation clearly needs to be further validated *in vivo*, and its exact mechanisms merit further exploration. The main findings of the current study are that after administration of NP, SC autophagy activity is elevated *in vitro* and in testis of rats. Furthermore, we consider that NP exposure elicits AMPKα phosphorylation and inhibits TSC2-mTOR signaling, resulting in autophagy induction and p70S6K/4EBP1 dephosphorylation in SCs.

Our previous in vivo study showed that NP enhanced autophagy activity in the testis of immature rats (Huang et al. 2016). Moreover, significant decreases in sperm motility and androgen production were found in NP-treated adult rats (Duan et al. 2016a). Normal spermatogenic progression is highly dependent on microenvironment provided by SCs, and conversely, SC dysfunction causes alterations of testis differentiation and adult spermatogenesis, potentially leading to temporary or permanent infertility (Dong et al. 2015; Hai et al. 2014). We were interested to investigate the mechanism how NP interferes with SC activity related to spermatogenesis, such as autophagy. In adulthood, SCs are terminally differentiated with loss of proliferative activity, and the disruption of SC homeostasis has been considered to be a leading cause of reproductive dysfunction (Wakui et al. 2012). Therefore, we investigated the reproductive toxicology of NP using adult male rats as an experimental modal. The autophagic genes Beclin-1, Atg3, Atg5, Atg7 and Atg12 are responsible for autophagosome biogenesis. In particular, Beclin-1 is required for Atg5/Atg7-dependent and -independent autophagy (Kang et al. 2011). Moreover, the ratio of LC3-II/LC3-I is a well-established marker for the detection of autophagy

(Hernandez et al. 2015). In this study, we found that the significant increase in the expression level of above autophagy-related genes induced by excessive NP administration was paralleled by an increase Beclin-1 protein expression, as well as by an elevation in LC3-II/LC3-I ratio, reflecting activation of autophagy in the testis. Our previous work observed that NP induces cytoprotective autophagy in SCs *in vitro* (Duan et al. 2016c), yet whether NP-induced SC autophagy plays a cytoprotective or a cytotoxic role in testis development and function still remains elusive.

Recent advances have shed new light on AMPK signaling both as a multitask gatekeeper and as an energy regulator (Mounier et al. 2015). Furthermore, More recent evidence highlights that the TSC2-mTOR signaling feeds into the AMPK pathway (Kim et al. 2016; Tanwar et al. 2012; Zhao et al. 2015). The present study revealed that treatment of NP robustly phosphorylated and activated AMPK, and simultaneously suppressed TSC2 and mTOR activity in testis. mTOR has been recognized as a central controller for cell growth and survival because of its important role in regulating multiple cellular processes, in particular protein synthesis as well as autophagy (Xu et al. 2014). Noteworthy, previously we showed up-regulation of AMPK as well as down-regulation of TSC2 and mTOR phosphorylation in NP-treated SCs (Duan et al. 2016c). Based on these findings, we assume that NP-induced SC autophagy is preceded by the AMPK-mTOR axis. p70S6K and 4EBP1 phosphorylation are responsible for ribosome recruitment to mRNA during the initiation phase of translation (Wang et al. 2014a). Especially, inhibition of mTOR blocks translation initiation and cell cycle progression and, consequently, affects cell growth and proliferation by phosphorylating its targets p70S6K and 4EBP1 (Wang et al. 2014a). The results from our previous in-vitro and present in-vivo studies revealed that NP exposure dephosphorylates p70S6K and 4EBP1, probably blocking protein synthesis, and therefore affecting testicular cell function and even spermatogenesis (Busada et al. 2015; Duan et al. 2016c).

Autophagy can be triggered through multiple interconnected pathways with the mTOR and AMPK cascades (Liang et al. 2015). Our previous research has revealed that the AMPK-mTOR-autophagy signaling cascade in SCs is reversed by the combination of the autophagy inhibitor 3-methyladenine and NP (Duan et al. 2016c). At this point a new questions that arises from this research is as follows: Whether AMPK is the critical upstream signaling that regulates mTOR and autophagy in NP-treated SCs. Altogether both pharmacological and siRNA strategies allow us to investigate the interactions between AMPK and mTOR underlying NP-triggered autophagy. Herein, experiments employing pharmacological and siRNA agents revealed that AMPK activation is crucial for the NP-induced SC autophagy. Interestingly, we also identified that AMPK signaling is responsible for NP-induced mTOR inhibition in SCs. AMPK has been shown to dephosphorylate TSC2, which inhibits mTOR activity and stimulates autophagy (Tanwar et al. 2012; Wu et al. 2015; Xu et al. 2014). As in our study, specifically inducing activation of AMPK with AICAR further decreased the phosphorylation of TSC2 in NP-treated SCs, whereas pharmacological blockade and siRNA-mediated knockdown of AMPK inhibited it. Collectively, the above evidence suggests that AMPK signaling negatively regulates mTOR activity by dephosphorylating TSC2, leading to induction of SC autophagy in response to NP exposure.

Both p70S6K and 4EBP1which are the major downstream effectors of mTOR are regulators of mRNA translation and protein synthesis involved in cell growth, cell survival, and apoptosis (Chang et al. 2015). Our early work showed that NP treatment induces cell necrosis and apoptosis, augments

AMPK activity and simultaneously inhibits p70S6K/4EBP1 phosphorylation (Duan et al. 2016c). To further clarify the mechanism of effect of NP, we checked whether the inhibitory effect of NP on 4EBP1 and p70S6K is dependent on the activity of AMPK signaling. In the present study, we found that NP-induced dephosphorylation of p70S6K and 4EBP1 was completely blocked by specific inhibitor (Compound C and AMPKα1 siRNA), implying that AMPK functions as a master upstream regulator, regulating p70S6K/4EBP1 activity. Importantly, NP-induced changes in AMPK-mediated inhibition of p70S6K/4EBP1 signaling possibly contributes to testicular toxicity in mammals, such as seminiferous tubule degeneration and a decrease in the number of spermatogenic cells. An interesting fact, although poorly understood, is that pharmacological activation of AMPK using AICAR failed to significantly affect NP-induced dephosphorylation of p70S6K/4EBP1. In this regard, we hypothesize that NP-induced autophagy is mostly independent of p70S6K and 4EBP1. In addition, the induction of P70S6K/4EBP1-mediated translation signaling is not always accordance with the expression of mTOR. This is a very interesting idea that merit to be investigated in future.

In summary, our study provides strong evidence that NP stimulates autophagy and suppresses mTOR-p70S6K/4EBP1 phosphorylation via AMPK phosphorylation in SCs. Pre-treatment with Compound C or siRNA-AMPKα1 effectively blocked NP-induced activation of AMPK, enabling the inhibition of SC autophagy as well as the restoration of the TSC2, mTOR, p70S6K and 4EBP1 phosphorylation. Conversely, pharmacological (AICAR) activation of AMPK significantly enhanced NP-induced SC autophagy through AMPK-mTOR pathway. These results offer new insights into the potential mechanisms responsible for testicular dysfunction caused by NP exposure. However, the detailed role of NP-induced SC autophagy and suppression of mTOR-p70S6K/4EBP1 pathways in the regulation of spermatogenesis needs to be elucidated.

Acknowledgments

Compliance with ethical standards

Conflict of interest None.

References

Albert, V., Hall, M.N. 2015. mTOR signaling in cellular and organismal energetics. Curr Opin Cell Biol. 33, 55-66.

Busada, J.T., Niedenberger, B.A., Velte, E.K., et al., 2015. Mammalian target of rapamycin complex 1 (mTORC1) Is required for mouse spermatogonial differentiation in vivo. Dev Biol. 407(1), 90-102.

Chang, X., Zhao, Y., Guo, L. 2015. Effect of Orexin-A on Cortisol Secretion in H295R Cells via p70S6K/4EBP1 Signaling Pathway. Int J Endocrinol. 2015, 405157.

Chen, M., Tang, R., Fu, G., et al., 2013. Association of exposure to phenols and idiopathic male infertility. J Hazard Mater. 250-251, 115-21.

Choi, M.S., Park, H.J., Oh, J.H., Lee, E.H., Park, S.M., Yoon, S. 2014. Nonylphenol-induced apoptotic cell death in mouse TM4 Sertoli cells via the generation of reactive oxygen species and activation of the ERK signaling pathway. J Appl Toxicol. 34(6), 628-36.

Churchward-Venne, T.A., Burd, N.A., Phillips, S.M. 2012. Nutritional regulation of muscle protein synthesis with resistance exercise: strategies to enhance anabolism. Nutr Metab (Lond). 9(1), 40.

Dong, H., Chen, Z., Wang, C., et al., 2015. Rictor Regulates Spermatogenesis by Controlling Sertoli Cell Cytoskeletal Organization and Cell Polarity in the Mouse Testis. Endocrinology. 156(11), 4244-56.

Duan, P., Hu, C., Butler, H.J., et al., 2016a. 4-Nonylphenol induces disruption of spermatogenesis associated with oxidative stress-related apoptosis by targeting p53-Bcl-2/Bax-Fas/FasL signaling. Environ Toxicol.

Duan, P., Hu, C., Butler, H.J., et al., 2016b. Effects of 4-nonylphenol on spermatogenesis and induction of testicular apoptosis through oxidative stress-related pathways. Reprod Toxicol. 62, 27-38.

Duan, P., Hu, C., Quan, C., et al., 2016c. 4-Nonylphenol induces apoptosis, autophagy and necrosis in Sertoli cells: Involvement of ROS-mediated AMPK/AKT-mTOR and JNK pathways. Toxicology. 341-343, 28-40.

Escott, G.M., da Rosa, L.A., Loss Eda, S. 2014. Mechanisms of hormonal regulation of sertoli cell development and proliferation: a key process for spermatogenesis. Curr Mol Pharmacol. 7(2), 96-108.

Gong, Y., Wu, J., Huang, Y., Shen, S., Han, X. 2009. Nonylphenol induces apoptosis in rat testicular Sertoli cells via endoplasmic reticulum stress. Toxicol Lett. 186(2), 84-95.

Guerrero-Bosagna, C., Skinner, M.K. 2014. Environmentally induced epigenetic transgenerational inheritance of male infertility. Curr Opin Genet Dev. 26, 79-88.

Hai, Y., Hou, J., Liu, Y., et al., 2014. The roles and regulation of Sertoli cells in fate determinations of spermatogonial stem cells and spermatogenesis. Semin Cell Dev Biol. 29, 66-75.

Han, S.P., Zhou, D.X., Lin, P., et al., 2015. Formaldehyde exposure induces autophagy in testicular tissues of adult male rats. Environ Toxicol. 30(3), 323-31.

Hardie, D.G. 2015. AMPK: positive and negative regulation, and its role in whole-body energy homeostasis. Curr Opin Cell Biol. 33, 1-7.

Hernandez, C., Barrachina, M.D., Vallecillo-Hernandez, J., et al., 2015. Aspirin-induced gastrointestinal damage is associated with an inhibition of epithelial cell autophagy. J Gastroenterol.

Huang, W., Quan, C., Duan, P., et al., 2016. Nonylphenol induced apoptosis and autophagy involving the Akt/mTOR pathway in prepubertal Sprague-Dawley male rats in vivo and in vitro. Toxicology 373:41-53.

Jesus, T.T., Oliveira, P.F., Silva, J., et al., 2015. Mammalian target of rapamycin controls glucose consumption and redox balance in human Sertoli cells. Fertil Steril.

Kang, R., Zeh, H.J., Lotze, M.T., Tang, D. 2011. The Beclin 1 network regulates autophagy and apoptosis. Cell Death Differ. 18(4), 571-80.

Kim, S.K., Kim, B.K., Shim, J.H., Gil, J.E., Yoon, Y.D., Kim, J.H. 2006. Nonylphenol and octylphenol-induced apoptosis in human embryonic stem cells is related to Fas-Fas ligand pathway. Toxicol Sci. 94(2), 310-21.

Kim, T.W., Kim, Y.J., Kim, H.T., et al., 2016. NQO1 deficiency leads enhanced autophagy in cisplatin-induced acute kidney injury through the AMPK/TSC2/mTOR signaling pathway. Antioxid Redox Signal.

Kim, Y.M., Jung, C.H., Seo, M., et al., 2015. mTORC1 phosphorylates UVRAG to negatively regulate autophagosome and endosome maturation. Mol Cell. 57(2), 207-18.

Kuo, P.L., Hsu, Y.L., Tsai, M.J., Lien, C.T., Huang, M.S., Ko, Y.C. 2012. Nonylphenol induces bronchial epithelial apoptosis via Fas-mediated pathway and stimulates bronchial epithelium to secrete IL-6 and IL-8, causing bronchial smooth muscle proliferation and migration. Basic Clin Pharmacol Toxicol. 110(2), 178-86.

Lepretti, M., Paolella, G., Giordano, D., et al., 2015. 4-Nonylphenol reduces cell viability and induces apoptosis and ER-stress in a human epithelial intestinal cell line. Toxicol In Vitro. 29(7), 1436-44.

Li, N., Mruk, D.D., Lee, W.M., Wong, C.K., Cheng, C.Y. 2016. Is toxicant-induced Sertoli cell injury in vitro a useful model to study molecular mechanisms in spermatogenesis? Semin Cell Dev Biol.

Liang, J., Xu, Z.X., Ding, Z., et al., 2015. Myristoylation confers noncanonical AMPK functions in autophagy selectivity and mitochondrial surveillance. Nat Commun. 6, 7926.

Liu, X., Nie, S., Huang, D., Xie, M. 2015. Mitogen-activated protein kinase and Akt pathways are involved in 4-n-nonyphenol induced apoptosis in mouse Sertoli TM4 cells. Environ Toxicol Pharmacol. 39(2), 815-24.

Lu, C., Zhang, F., Xu, W., et al., 2015. Curcumin attenuates ethanol-induced hepatic steatosis through modulating Nrf2/FXR signaling in hepatocytes. IUBMB Life. 67(8), 645-58.

Lu, W.C., Wang, A.Q., Chen, X.L., et al., 2014. 90d Exposure to Nonylphenol has Adverse Effects on the Spermatogenesis and Sperm Maturation of Adult Male Rats. Biomed Environ Sci. 27(11), 907-11.

Lyons, R., Van de Bittner, K., Morgan-Jones, S. 2014. Deposition patterns and transport mechanisms for the endocrine disruptor 4-nonylphenol across the Sierra Nevada Mountains, California. Environ Pollut. 195, 123-32.

McClusky, L.M., de Jager, C., Bornman, M.S. 2007. Stage-related increase in the proportion of apoptotic germ cells and altered frequencies of stages in the spermatogenic cycle following gestational, lactational, and direct exposure of male rats to p-nonylphenol. Toxicol Sci. 95(1), 249-56.

Mounier, R., Theret, M., Lantier, L., Foretz, M., Viollet, B. 2015. Expanding roles for AMPK in skeletal muscle plasticity. Trends Endocrinol Metab. 26(6), 275-86.

Qi, S., Fu, W., Wang, C., et al., 2014. BPA-induced apoptosis of rat Sertoli cells through Fas/FasL and JNKs/p38 MAPK pathways. Reprod Toxicol. 50, 108-16.

Reis, M.M., Moreira, A.C., Sousa, M., Mathur, P.P., Oliveira, P.F., Alves, M.G. 2015. Sertoli cell as a model in male reproductive toxicology: Advantages and disadvantages. J Appl Toxicol. 35(8), 870-83.

Riera, M.F., Regueira, M., Galardo, M.N., Pellizzari, E.H., Meroni, S.B., Cigorraga, S.B. 2012. Signal transduction pathways in FSH regulation of rat Sertoli cell proliferation. Am J Physiol Endocrinol Metab. 302(8), E914-23.

Song, Y., Liang, X., Hu, Y., Wang, Y., Yu, H., Yang, K. 2008. p,p'-DDE induces mitochondria-mediated apoptosis of cultured rat Sertoli cells. Toxicology. 253(1-3), 53-61.

Tanwar, P.S., Kaneko-Tarui, T., Zhang, L., Teixeira, J.M. 2012. Altered LKB1/AMPK/TSC1/TSC2/mTOR signaling causes disruption of Sertoli cell polarity and spermatogenesis. Hum Mol Genet. 21(20), 4394-405.

Verderame, M., Limatola, E. 2015. Interferences of an environmental pollutant with estrogen-like action in the male reproductive system of the terrestrial vertebrate Podarcis sicula. Gen Comp Endocrinol. 213, 9-15.

Vidal-Linan, L., Bellas, J., Salgueiro-Gonzalez, N., Muniategui, S., Beiras, R. 2015. Bioaccumulation of 4-nonylphenol and effects on biomarkers, acetylcholinesterase, glutathione-S-transferase and glutathione peroxidase, in Mytilus galloprovincialis mussel gilla. Environ Pollut. 200, 133-9.

Wakui, S., Muto, T., Suzuki, Y., et al., 2012. Sertoli cells proliferate in adult rats with prenatal exposure to 3,3',4,4',5-pentachlorobiphenyl. Arch Toxicol 86(1):159-62.

Wang, C., Yan, Y., Hu, L., et al., 2014a. Rapamycin-mediated CD36 translational suppression contributes to alleviation of hepatic steatosis. Biochem Biophys Res Commun. 447(1), 57-63.

Wang, Y., Zheng, W., Bian, X., et al., 2014b. Zearalenone induces apoptosis and cytoprotective autophagy in primary Leydig cells. Toxicol Lett. 226(2), 182-91.

Wu, J.C., Wang, F.Z., Tsai, M.L., et al., 2015. Se-Allylselenocysteine induces autophagy by modulating the AMPK/mTOR signaling pathway and epigenetic regulation of PCDH17 in human colorectal adenocarcinoma cells. Mol Nutr Food Res.

Xu, Y., Liu, C., Chen, S., et al., 2014. Activation of AMPK and inactivation of Akt result in suppression of mTOR-mediated S6K1 and 4E-BP1 pathways leading to neuronal cell death in in vitro models of Parkinson's disease. Cell Signal. 26(8), 1680-9.

Yamamoto, A., Mizushima, N., Tsukamoto, S. 2014. Fertilization-induced autophagy in mouse embryos is independent of mTORC1. Biol Reprod. 91(1), 7.

Yao, G., Hu, Y., Liang, J., Hou, Y. 2005. Nonylphenol-induced thymocyte apoptosis is related to Fas/FasL pathway. Life Sci. 77(26), 3306-20.

Yefimova, M.G., Messaddeq, N., Harnois, T., et al., 2013. A chimerical phagocytosis model reveals the recruitment by Sertoli cells of autophagy for the degradation of ingested illegitimate substrates. Autophagy. 9(5), 653-66.

Yue, Y., Wang, Y., Li, D., Song, Z., Jiao, H., Lin, H. 2015. A central role for the mammalian target of rapamycin in LPS-induced anorexia in mice. J Endocrinol. 224(1), 37-47.

Zhang, H., Ke, J., Shao, T., et al., 2014. Cytotoxic effects of procyanidins from Castanea mollissima Bl. shell on human hepatoma G2 cells in vitro. Food Chem Toxicol. 64, 166-76.

Zhao, P., Dou, Y., Chen, L., et al., 2015. SC-III3, a novel scopoletin derivative, induces autophagy of human hepatoma HepG2 cells through AMPK/mTOR signaling pathway by acting on mitochondria. Fitoterapia. 104, 31-40.
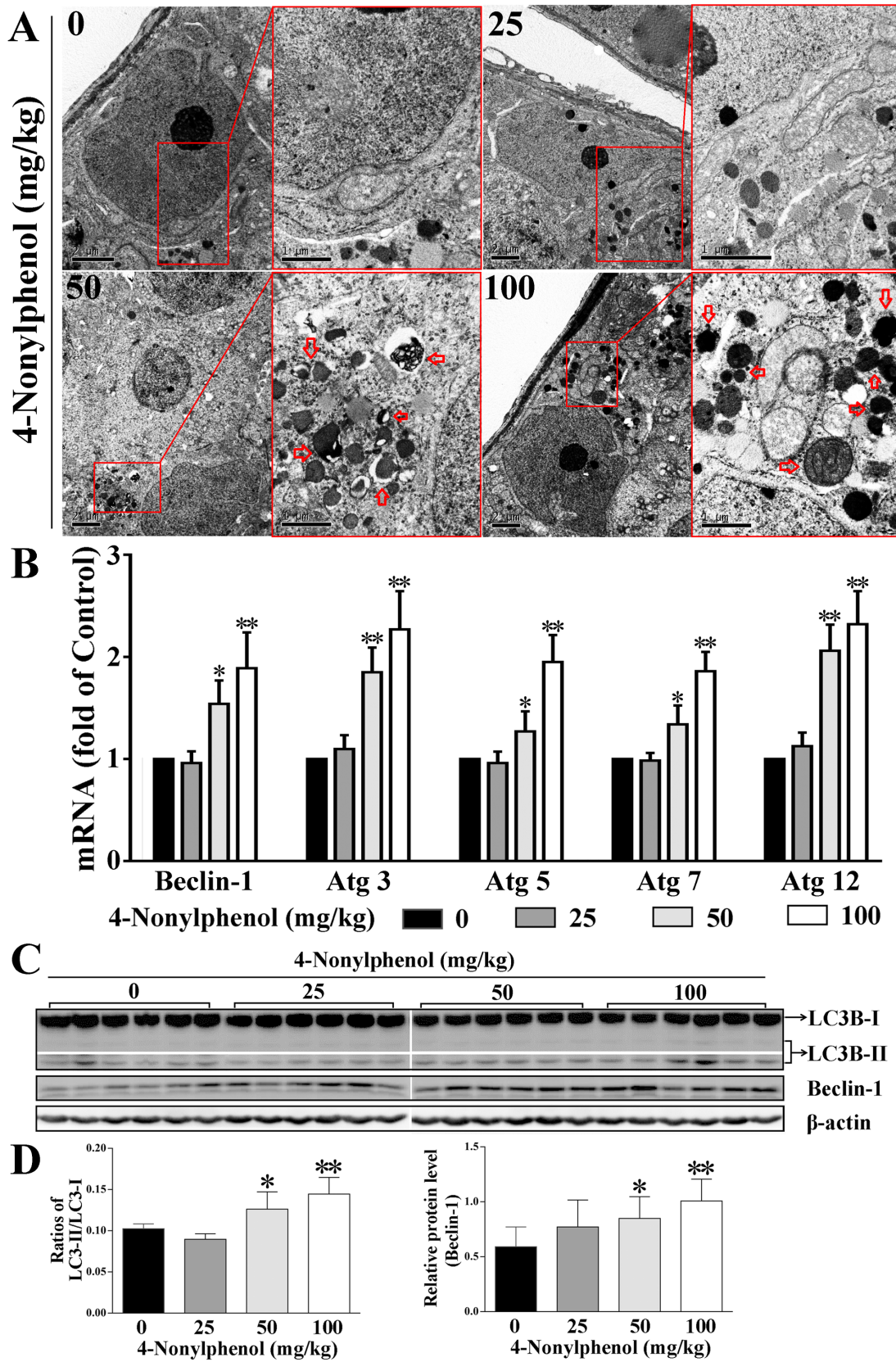
Fig.1. 4-nonylphenol induced Sertoli cell autophagy, which was coincidental with upregulation of autophagy-related proteins and genes expression in rat testis. (A) Transmission electron microscopic

evaluation of autophagosomes in Sertoli cells of testis in rats. The arrows indicate formed autophagosomes and autolysosomes. All images are representative of three rats per group. Scale bars: 2 μm and 1 μm. (B) Effect of 4-nonylphenol on mRNA levels of Beclin-1, Atg3, Atg5, Atg7 and Atg12 of testicular tissue, was assessed by real-time quantitative PCR. The data are relative mRNA level normalized to β-actin mRNA level. The normalised levels of the control mRNA are expressed as 1. (C) Protein expression of autophagy markers (LC3-II/LC3-I and Beclin-1) in testis were performed by Western blotting following 4-nonylphenol treatment. β-actin was used as the loading control. The immunoblots shown here are representative of three independent experiments with similar results. (D) Quantification showed significant increase of Beclin-1 and the conversion from LC3-I to LC3-II in 50-100 mg/kg groups. Each bar denotes mean ± SD of six rats. *$P<0.05$, **$P<0.01$ versus control group (without 4-nonylphenol treatment), one-way ANOVA.
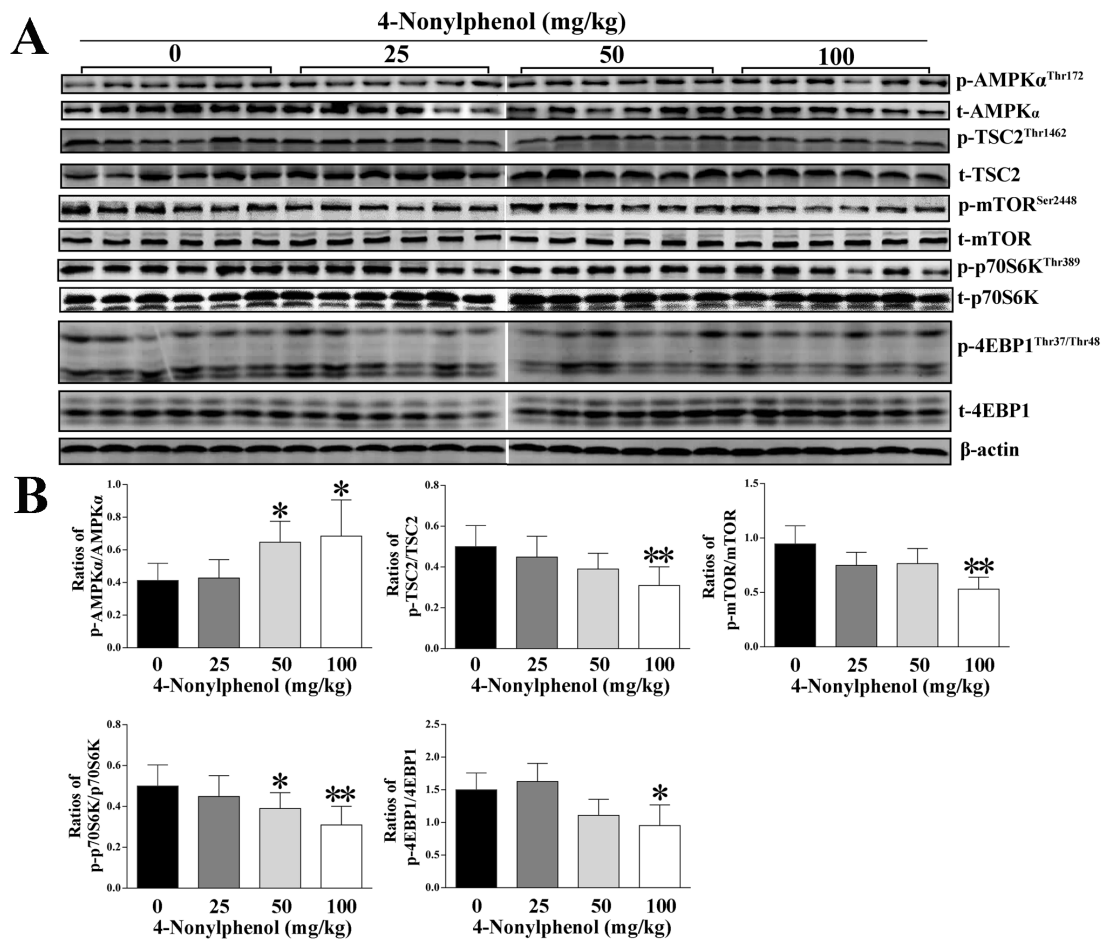

Fig.2. 4-nonylphenol potently activated AMPK and inhibited TSC2/mTOR/p70S6K/ 4EBP1 signaling in rat testis. (A) Western blots show the effects of 4-nonylphenol on the expression of p-AMPKα/AMPKα, p-TSC2/TSC2, p-mTOR/mTOR, p-p70S6K/p70S6K and p-4EBP1/4EBP1in testis. β-actin reprobing was used to control for protein loading. Blots are representative of three independent experiments. (B) Bar graph shows the quantification of the indicated proteins from the data shown in (A). β-actin was used as the loading control. Data are expressed as mean ± SD in each bar graph from
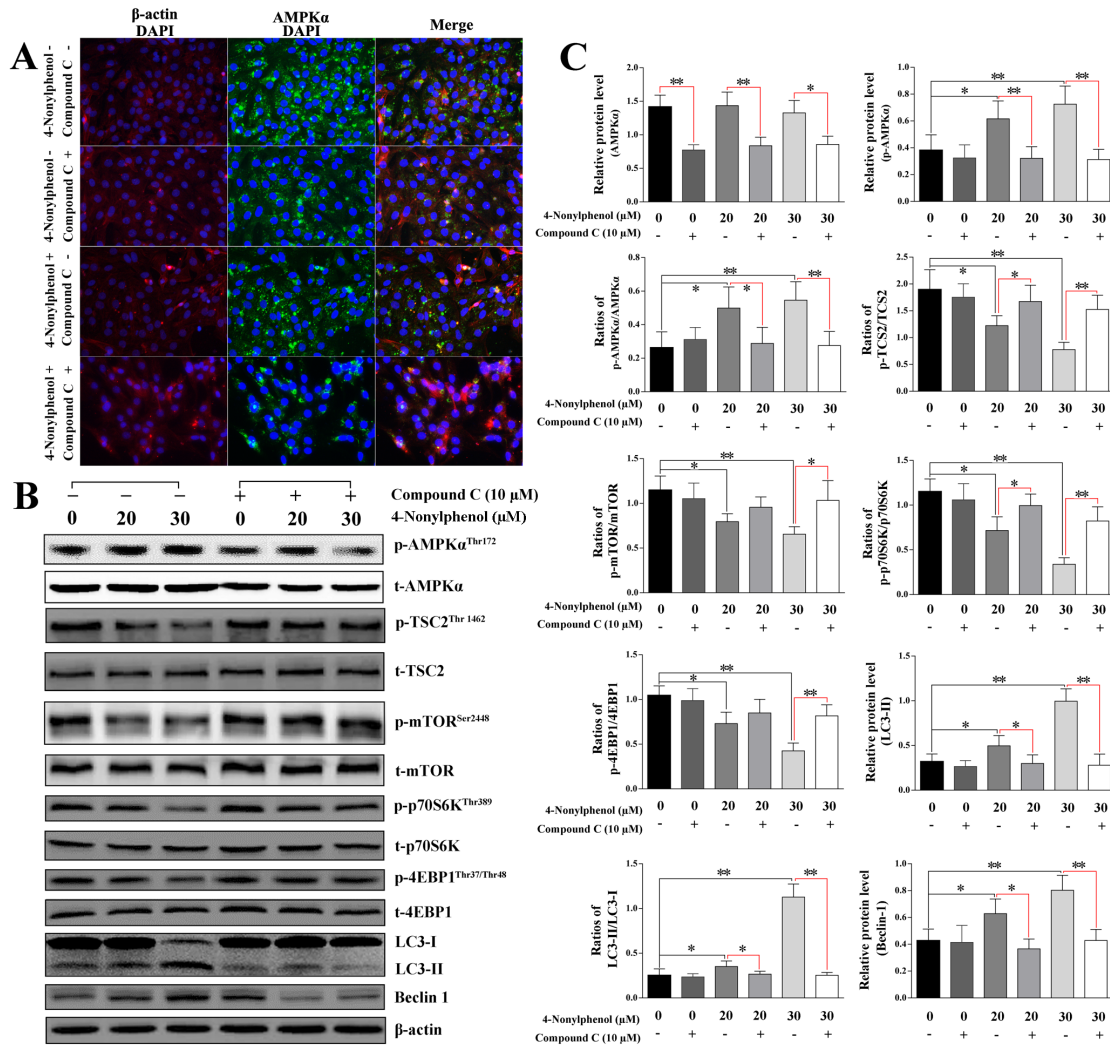
Fig.3. Pharmacological inhibition of AMPK using the AMPK inhibitor compound C abrogated 4-Nonylphenol induced-autophagy and -suppression of TSC2/mTOR/p70S6K/ 4EBP1 pathway in Sertoli cells. (A) Representative immunofluorescence staining showing expression of AMPKα protein in Sertoli cells treated with or without 20-30 μM 4-Nonylphenol in the presence or absence of compound C. AMPKα was stained with green fluorescence, β-actin was stained with red fluorescence, and nucleus was stained with DAPI (blue), ×400 magnification. (B) Representative immunoblots showing the effects of compound C on AMPK/TSC2/mTOR/ p70S6K/4EBP1 signaling and autophagy induction in 4-Nonylphenol-treated and -untreated cells. The internal control β-actin was used to normalize loading variations. (C) Bar plot showing the quantification of the protein expression levels in (B). Sertoli cells without any treatment serve as control. Cells treated with only compound C were used as positive control. All data are presented as mean ± SD of three experiments. *$P < 0.05$, **$P < 0.01$ significantly different from the corresponding group.
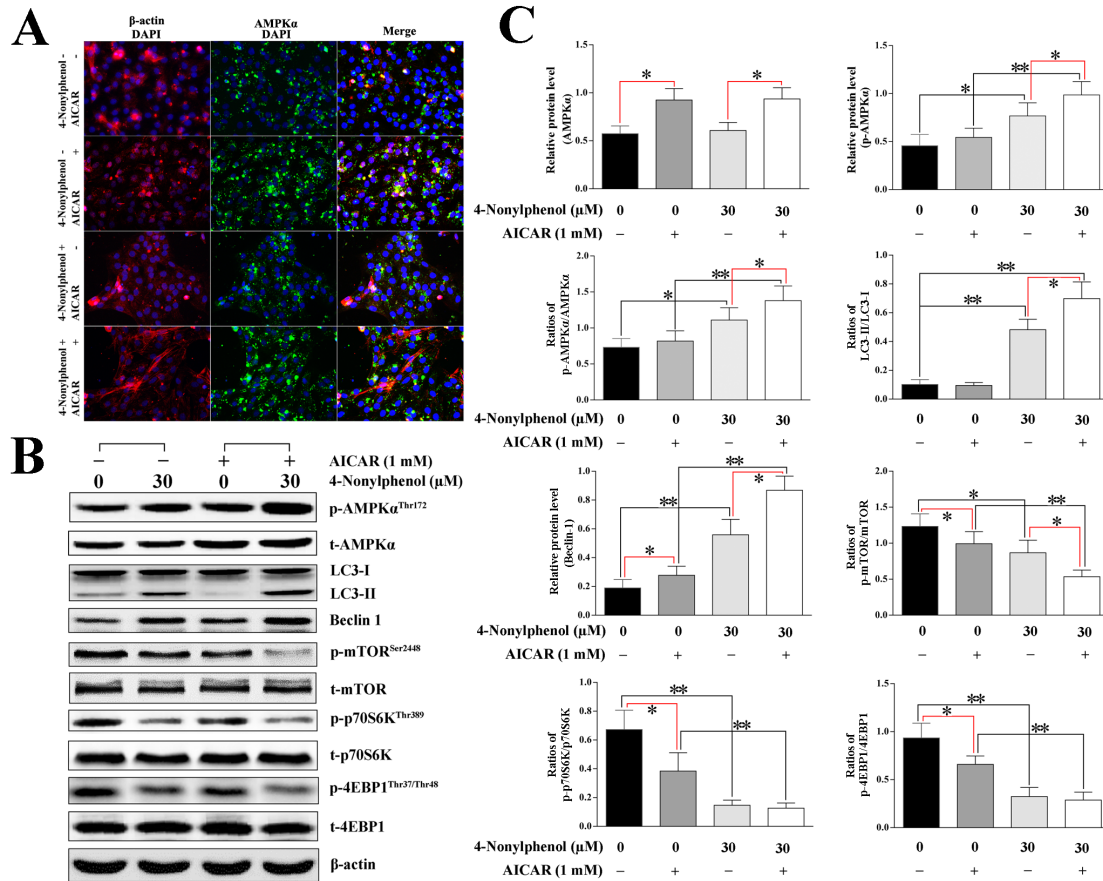
Fig.4. The pharmacological activation of AMPK using AICAR (an AMPK activator) exacerbated 4-Nonylphenol-induced autophagy and further inhibited mTOR signaling. (A) Representative immunofluorescence images showing the expression of AMPKα protein (green), β-actin (red), and nuclei DAPI staining (blue) in Sertoli cells after indicated treatments. Images are shown at 400× magnification. (B) Representative immunoblots showing the effects of AICAR on the expression of LC3-II/LC3-I and Beclin-1 and on AMPK/mTOR pathway in 4-Nonylphenol-treated and -untreated cells. β-actin is the loading control. The results were representative of three independent experiments. (C) Bar plot showing the quantification of the protein expression levels in (A). Sertoli cells without any treatment serve as control. Cells treated with only AICAR were used as positive control. The results were presented as mean ± SD. *$P < 0.05$, **$P < 0.01$ significantly different from the corresponding group.
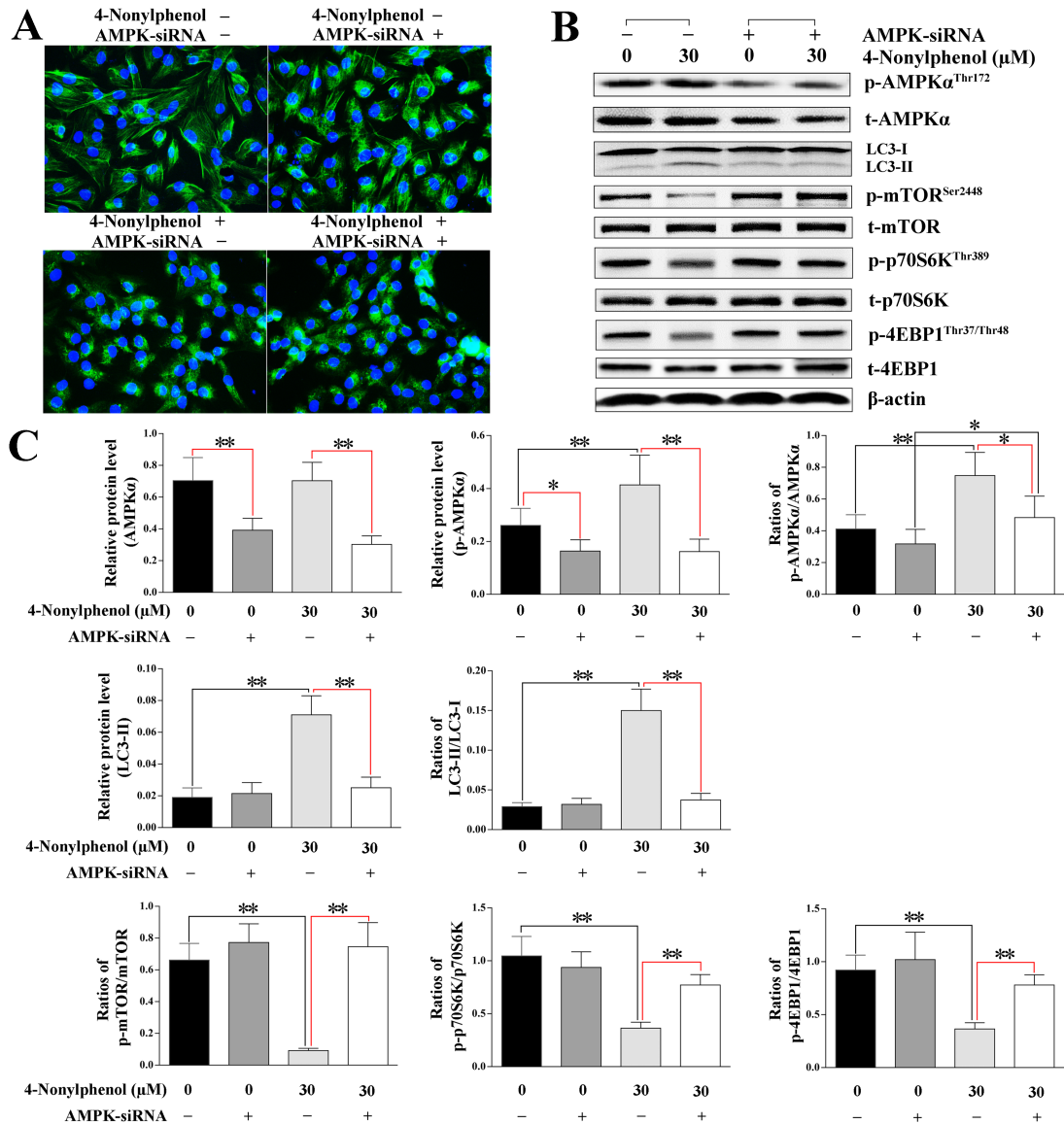
Fig.5. Silencing of AMPKα blocked 4-Nonylphenol-induced autophagy induction and mTOR/p70S6K/4EBP1 signaling inhibition in Sertoli cells. (A) Effects of AMPKα1 siRNA transfection on the cytoskeleton and morphology of Sertoli cells. The F-actin cytoskeleton (Phalloidin staining) was visualized in green and cell nucleus (DAPI staining) was stained in blue. Representative images of each group are depicted (400× magnification). (B) Representative immunoblots showing the effects of AMPKα knockdown on the expression of LC3-II/LC3-I and Beclin-1 and on mTOR/p70S6K/4EBP1 pathway in 4-Nonylphenol-treated cells. β-actin served as a loading control. (C) Bar plot showing the quantification of the protein expression levels in (B). Sertoli cells without any treatment serve as control. Cells treated with siRNA against AMPKα were used as positive control. Western blots and bar charts are representative of at least independent 3 experiments. The results were presented as mean ± SD. *$P < 0.05$, **$P < 0.01$ significantly different from the corresponding group.